

OPTICAL ELEMENTS

https://doi.org/10.1070/QEL16336

Effect of structural defects of aperiodic multilayer mirrors on the properties of reflected (sub)femtosecond pulses

S.A. Garakhin, E.N. Meltchakov, V.N. Polkovnikov, N.N. Salashchenko, N.I. Chkhalo

Abstract. **The effect of structural defects (for example, of interlayer roughness, layer thickness fluctuations and departures of Mo film density from the tabular one) on the amplitude and phase of the complex reflection coefficient as well as on the amplitude and duration of reflected pulses is numerically studied by the example of a model aperiodic Mo/Si multilayer mirror intended for the compression of a chirped pulse with a spectrum lying in a 50–80 eV photon energy range. The departures of Mo film density from the tabular values and film thickness fluctuations are shown to exert the strongest effect on the amplitude and duration of the reflected pulses. The interlayer roughness has a comparable effect on the amplitude of the reflection coefficient, but its effect on the duration of reflected pulses is weaker. Even small film thickness fluctuations may give rise to additional reflected pulses of high intensity, which are delayed in time relative to the principal pulse. The Mo-film density in a Mo/Si mirror is shown to vary from 0.77 to 0.97 (in units of the tabular value for massive molybdenum) as the film thickness varies from 1.5 to 5.5 nm. We discuss the key problems that have to be solved in the development of the fabrication technology of multilayer mirrors with desired characteristics.**

Keywords: *aperiodic multilayer mirror, chirped femtosecond pulse, complex reflection coefficient, genetic algorithm, roughness, Fourier transform.*

1. Introduction

In connection with the recent progress in the development of high-power femtosecond lasers, great interest is being shown in the generation of (sub)femtosecond and attosecond pulses of electromagnetic radiation. Such pulses may be obtained, for instance, in the coherent generation of high-order harmonics of laser radiation [1], in the coherent interaction of laser radiation with relativistic charged-particle beams [2], and in the interaction of femtosecond laser beams with solids [3]. Since the pulse duration turns out to be comparable to the electron 'revolution period' in atoms, to the times of interatomic, intraatomic, and, in some cases, intranuclear transitions, this radiation may become a unique instrument in studies of fast processes [4–6].

Another no less important application of attosecond pulses is the production of ultrahigh electromagnetic fields and, accordingly, of extremely high power densities. As shown by the estimates made in Ref. [7], even with the use of a FLASH free-electron laser with a relatively low peak power [8], a pulse duration of 250 fs, and a pulse energy of only 1.4 mJ at a wavelength of 13.5 nm it is possible to achieve an intensity of over 10^{21} W cm^{-2} at the focus of normal-incidence multilayer mirrors. This takes place due to nanofocusing (the diffraction-limited focal spot diameter in the 10-nm domain is approximately two orders of magnitude smaller and the area is therefore four orders of magnitude smaller than in the IR domain) and the short pulse duration. In modern high-power lasers the pulse energy amounts to tens of joules and the pulse duration may be as short as several femtoseconds [3]. In view of efficient conversion of the energy of laser pulses to the energy of (sub)femtosecond and attosecond pulses [9], even at the modern level of technology one might expect the generation of (sub)femto- and attosecond pulses producing at-focus intensities of up to 10^{28} W cm^{-2}, which is close to the threshold intensity of vacuum 'breakdown'.

The successful solution of this task faces the problem of manipulating these pulses (transportation, collimation and focusing of the beams, spectral analysis, control of the spectrum etc.). Since the spectral width Δf of a pulse of duration τ_0 satisfies the inequality $\Delta f \geqslant 1/\tau_0$, its spectrum lies in the domain of extreme UV (EUV) and soft X-ray radiation. For a duration $\tau_0 = 1$–100 as, the frequencies lie in the range 10^{16}–10^{18} Hz and the wavelengths lie in the range 0.3–30 nm. The authors of several papers showed that periodic and aperiodic multilayer mirrors (PMMs and AMMs) are among the most efficient optical elements suited to the solution of these tasks [10–13]. The choice of the multilayer mirror type is determined both by the duration of a pulse and by its carrier frequency. As emphasised in Ref. [14], for pulses shorter than 1 fs and the carrier frequency corresponding to a photon energy of 77.6 eV, for instance, the pulse spectrum is broader than the reflection spectrum of a Mo/Si PMM, with the effect that the reflection efficiency of this structure is lowered. That is why of interest for the majority of applications are AMMs, for which the spectral width of the high reflectivity domain may be several times broader than for PMMs.

However, a broad reflection spectrum alone does not solve the problem of reflecting short pulses without distorting their frequency and time characteristics. In the passage of radiation through a multilayer mirror, different spectral components penetrate to different depths owing to dispersion of optical

S.A. Garakhin, V.N. Polkovnikov, N.N. Salashchenko, N.I. Chkhalo Institute for Physics of Microstructures, Russian Academy of Sciences, ul. Akademicheskaya7, 603087 Afonino, Kstovskii raion, Nizhnii Novgorod region, Russia; e-mail: polkovnikov@ipmras.ru;
E.N. Meltchakov Laboratoire Charles Fabry, Institut d'Optique Graduate School, 2 av. Augustin Fresnel, 91127 Palaiseau, France

Received 3 March 2017
Kvantovaya Elektronika **47** (4) 378–384 (2017)
Translated by E.N. Ragozin

constants (as a rule, high-frequency components penetrate deeper into the structure), thereby giving rise to an additional phase difference between the reflected spectral components. This results in a pulse spreading. That is why in the structure optimisation of an AMM intended for controlling a pulse with preselected characteristics it is required to take into account not only the amplitude but also the phase of all spectral components. Numerous papers are concerned with the calculations of AMMs intended for the reflection of (sub)femto- and attosecond pulses. Calculations were made for pulses with a fixed carrier frequency as well as for chirped pulses (varied carrier-frequency pulses). In the former case, the task was set to retain the reflected pulse shape, and so the objective was to make equal the amplitudes and phases of the reflection coefficients of all spectral components. For chirped pulses, whose carrier frequency varied according to a specific law under the enveloping curve [15], the task was set to shorten the pulse duration. In the formulation of the objective function, additional conditions were therefore imposed on the amplitude and phase of the reflection coefficient, which are considered below.

The main drawback of the works mentioned above is that the calculations were made for AMMs with perfect structure parameters: zero interlayer roughness, tabular densities, and nominal film thicknesses. These conditions are not fulfilled in practice. Furthermore, the film material densities may depend on film thickness. As shown earlier in Ref. [16], which analysed the effect of interlayer roughness, film densities, random and systematic film errors on the spectral dependence of the AMM reflection coefficient, the inclusion of these structural defects leads to optimal AMM film layer thicknesses, which are different from the 'ideal' case. Conversely, the use of an AMM structure obtained by neglecting the roughness and real film material densities results in a strong distortion of the spectral dependence of reflectivity in comparison with the requisite one.

Here, by the example of a 1-fs long chirped pulse with a carrier frequency corresponding to a photon energy of 70 eV, for the first time we performed a numerical analysis of the influence of structural Mo/Si AMM defects (interlayer roughness, departure of film densities from their tabular data, film thickness fluctuations) on the amplitude and duration of the reflected pulse. Reported for the first time is the measured dependence of molybdenum film density in Mo/Si mirrors on the film thickness, which is varied over a wide range typical for AMMs. We discuss the main problems which should be solved for improving AMM structure optimisation algorithms in the solution of specific problems of (sub)femto- and attosecond electromagnetic pulse control. The treatment of chirped pulses in our paper is caused only by the authors' practical interest towards the possibility of pulse compression and does not affect the generality of the result. Similar results would have also been obtained in the treatment of the effect of structural AMM defects on pulses with a constant carrier frequency.

2. Technique for designing AMMs intended for chirped-pulse compression

The method for calculating the shape of reflected pulses is based on Fourier transforms. At first the direct Fourier transform yields the spectrum of the incident wave. Next the spectrum is multiplied by the complex reflection coefficient of the mirror, and subsequently the reflected pulse is found using the inverse Fourier transform.

At present there is no direct access to the software which makes it possible to design the structure composition optimised to yield the prescribed shape of reflected pulses. And so, following the authors of Ref. [17], for the solution of this problem we defined two goal functions: the profiles of amplitude and phase of the reflection coefficient throughout the pulse spectrum. The calculations were performed using the IMD code [18]. At the first stage, selected for a goal profile for the reflectivity amplitude was a rectangular profile (a plateau) bounded by the photon energies $\varepsilon_{\min}$ and $\varepsilon_{\max}$, while the AMM layer thicknesses were treated as fitting parameters. These calculations were made for the Mo/Si AMM most often used in the EUV range. Furthermore, the number of bilayers in the sample was an additional fitting parameter. The first (counting from the substrate) layer was composed of silicon and the last one of molybdenum. An Mo/Si PMM with a reflectivity peak at a frequency ω_0 was the initial structure for the first step.

At the next stage, adopted for the second goal profile was a quadratic dependence of the phase of the amplitude reflection coefficient on the photon energy. As shown in Ref. [17], the quadratic energy dependence of the phase permits selecting the AMM parameters whereby the reflected pulse is compressed in time, the compression ratio ranging up to 10 in this case.

As a rule, the reflectivity plateau of the structure was distorted after the optimisation phase. Therefore, the next step involved correction of the plateau. The structure obtained in the previous stage was the starting point for this step. After each cycle of AMM structure optimisation in reflectivity and phase we checked the shape of the reflected pulse using the Fourier transform. The procedure of optimising the amplitude and phase of the reflection coefficient was repeated until the reflected pulse duration reached the prescribed value or ceased to vary.

For definiteness we address ourselves to the problem of compressing a 1-fs long pulse with an amplitude E_0 (Fig. 1). We consider the case when the phase of a Gaussian pulse varies in time according to a quadratic law:

$$E(t) = E_0 \exp[-\Gamma t^2 + \mathrm{i}(\omega_0 t - at^2)], \qquad (1)$$

where the enveloping curve shape is determined by the duration τ_0 defined at a 10% level of the pulse amplitude, the

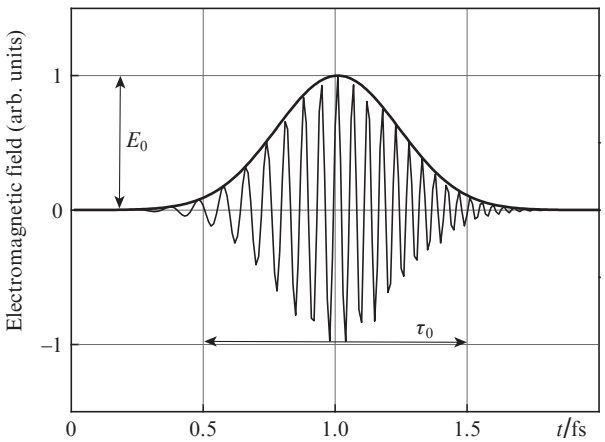

Figure 1. Initial chirped Gaussian pulse of amplitude E_0 and duration τ_0. The pulse duration is defined at a 10% level of the peak field magnitude.

coefficient $\Gamma = \tau_0^{-2}$, and the quantity a, which characterises the chirp parameter. In our case, $\tau_0 = 1$ fs and $a = 10$ fs^{-2}.

The outcome was a calculated AMM structure, which corresponded nicely to both goal profiles. Figure 2 shows the dependences of Mo and Si layer thicknesses on the layer number (the layers are numbered from the surface to the substrate) for this AMM. The Mo and Si layer thicknesses lie in the ranges 2.1–5.2 nm and 3.9–8.7 nm, respectively, and the number of bilayers is equal to 80. Figure 3 shows the spectra of the squared amplitude and phase of the reflection coefficient of a perfect (devoid of structural defects) Mo/Si AMM calculated by the method described above. One can see that the average reflectivity is equal to about 15%, and the reflectivity plateau is strongly distorted in the low-energy domain in this case. The energy dependence of the phase of the reflection coefficient is close to a quadratic one.

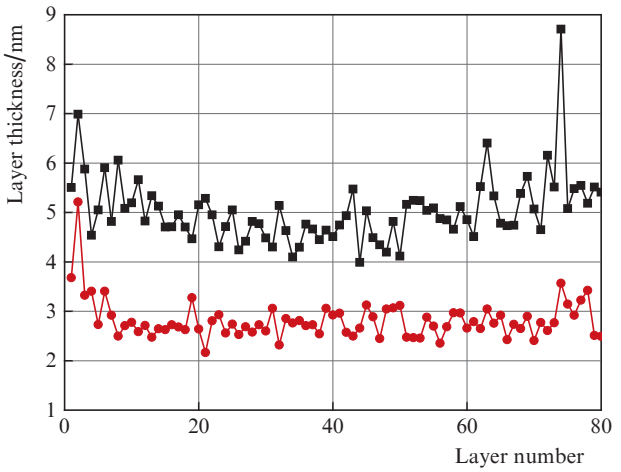

Figure 2. Mo (●) and Si (■) layer thicknesses in relation to the layer number of the optimised AMM.

The pulse incident on the designed AMM and the reflected pulse are compared in Fig. 4. In the incidence of a 1-fs long pulse with an amplitude E_0 the pulse reflected from the AMM has an amplitude equal to $0.57E_0$ and a duration of 0.24 fs. Therefore, even for an average energy reflectivity of 15%, the

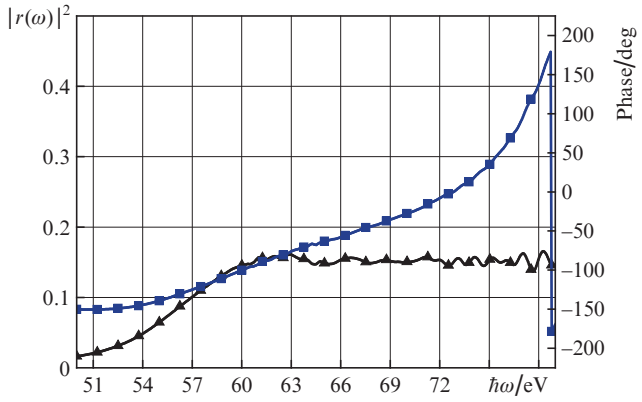

Figure 3. Squared amplitude $|r(\omega)|^2$ (▲) and phase (■) of the reflection coefficient of the Mo/Si AMM optimised for maximum uniform reflectivity in the 60–80 eV range in the compression of a chirped pulse.

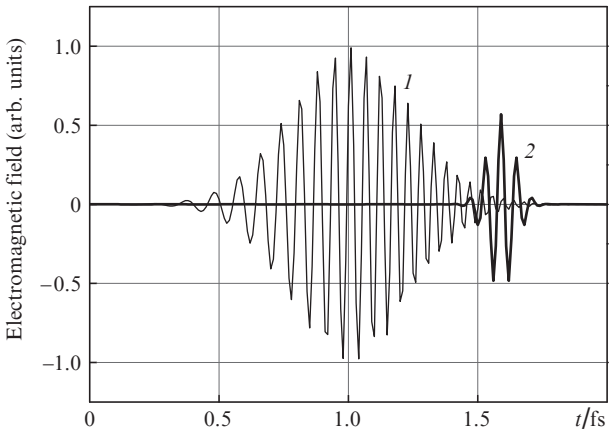

Figure 4. Comparison of the fields of the pulse (*1*) incident on the perfect AMM and the reflected pulse (*2*).

amplitude of the reflected pulse amounts to 57% of the amplitude of the incident one due to a four-fold pulse shortening. In this case, the power of electromagnetic field increased by more than two times.

3. Influence of structural AMM defects on the reflection coefficient and the characteristics of reflected pulses

There is no way of fabricating an AMM with a perfect structure: random layer thickness departures (fluctuations) from design values will inevitably occur in reality. Furthermore, in a real multilayer structure there are interlayer transition boundaries, which will be referred to as roughness, and the film have densities different from the tabular ones. As noted in the foregoing, the authors of Ref. [16] considered the effect of deterministic and random departures of layer thicknesses from their nominal values as well as of interlayer roughness on the spectral dependence of AMM reflectivity. They showed that these defects exert an appreciable effect on the shape of the spectral reflectivity curve and should be taken into account in the calculation of AMM structure. In this Section we consider the effect of internal AMM structure defects like variations of molybdenum film density, interlayer roughness and thickness fluctuations on the amplitude and phase characteristics of the reflection coefficient as well as on the amplitude and duration of reflected pulses.

3.1. Effect of roughness

The root-mean-square roughness of periodic Mo/Si mirrors optimised for the EUV range has been adequately studied [19, 20]. Practically all investigations suggest that the Mo-on-Si boundary roughness is equal to 12 nm and the Si-on-Mo boundary roughness is equal to 0.6 nm. In the subsequent calculations we used these values.

Figures 5a and 5b show the calculated spectral dependences of the squared amplitude and phase of the reflection coefficient for the AMM whose layer thicknesses are depicted in Fig. 2. With reference to Fig. 5a, in good agreement with the calculations of Ref. [16] the roughness is responsible for a lowering of the reflectivity as well as for a change in the shape of the spectral dependence of the reflectivity. In this case, as

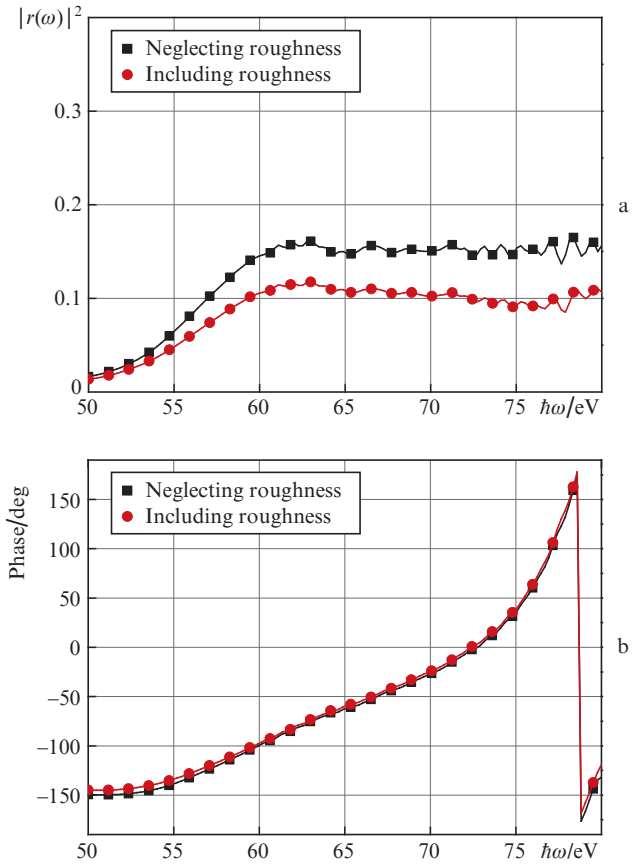

Figure 5. Effect of interlayer roughness (0.6 nm for the Si-on-Mo interface and 1.2 nm for the Mo-on-Si interface) on the squared amplitude (a) and phase (b) of the complex reflection coefficient of the AMM.

suggested by Fig. 5b, the roughness has only an insignificant effect on the phase of the reflection coefficient.

The reflected pulse has a slightly longer duration and a one-and-a-half times lower amplitude than the pulse reflected from the perfect structure: 0.28 fs and $0.39E_0$, respectively (Table 1). Therefore, the roughness affects mostly the amplitude of reflected wave and has a considerably smaller effect on the pulse duration.

Table 1. Effects of roughness, random spread of layer thicknesses, and departure from the tabular Mo layer density on the main parameters of reflected pulses.

Structural defects	Field amplitude	Duration/fs
Perfect structure	$0.57E_0$	0.24
Roughness	$0.39E_0$	0.28
Random thickness spread	$0.37E_0$	0.35
Departure of Mo film density from the tabular one	$0.33E_0$	0.31

3.2. Effect of film thickness fluctuations

The second factor which affects the parameters of reflected pulses is the random errors (fluctuations) of the film thicknesses in AMMs. Practice suggests that random errors in the application of magnetron sputtering technology are due to fluctuations of the voltage across the magnetron, of discharge current, and the pressure of the working gas.

To simulate this effect in the performance of calculations by the IMD code, use was made of function of the following form:

$$z_j' = z_j + \delta z \cdot \mathrm{RANDOM(seed)}, \qquad (2)$$

where z_j is the nominal jth layer thickness in the AMM; the RANDOM(seed) operator obeys the normal distribution with the zero average value and unit standard deviation; the parameter $\delta z = 0.1$ nm (this value is typical for PMM deposition by magnetron sputtering technique). The root-mean-square roughness of the interlayer boundaries was assumed to be zero.

Figures 6a and 6b show the calculated effect of layer thickness fluctuations on the amplitude and phase characteristics of AMM reflection coefficients. Plotted in the drawings for clearness are characteristic (selected out of two hundred) realisations corresponding to 'out-of-order' curves and to the case of greatest crowding of the curves. Since the realisation probability of extreme variants, which exert the greatest effect on the spectrum, is low, we adopted precisely the medium case to analyse the effect of thickness fluctuations on the parameters of reflected pulses. It is noteworthy that thickness fluctuations have a significant effect both on the amplitude and on the phase of the complex reflection coefficient, which eventually affects the amplitude and duration of reflected pulses: $0.37E_0$ and 0.35 fs, respectively (Table 1). Therefore,

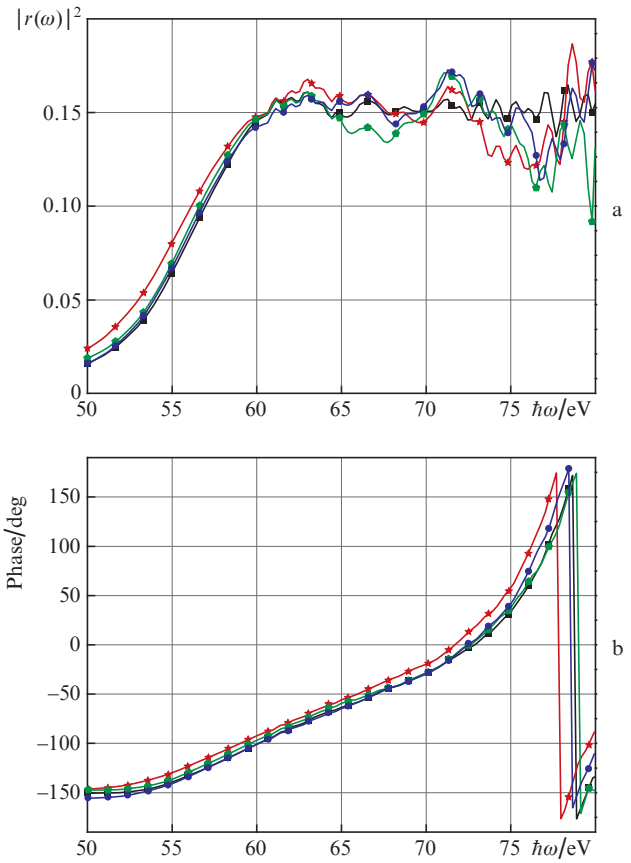

Figure 6. (Colour online) Effect of film thickness fluctuations on the amplitude and phase characteristics of AMM reflection coefficient. We show the characteristic realisations corresponding to 'out-of-order' curves and to the case of their greatest crowding. The curve with square symbols corresponds to a medium realisation.

thickness fluctuations play a role of greater significance than roughness, especially so from the viewpoint of the duration of reflected pulses.

Strictly speaking, the field magnitude at a level of 10% of the amplitude of the reflected pulse is reached at several points in time, so strong is the time spreading of the signal. This is seen in Fig. 7. A value of 0.35 fs was taken for the first crossing of the pulse envelope with the level equal to 10%. Layer thickness fluctuations result in the spreading of reflected pulses. The signal duration increases significantly and the peak power decreases. This is the most grave implication of the thickness fluctuations of AMM constituent layers.

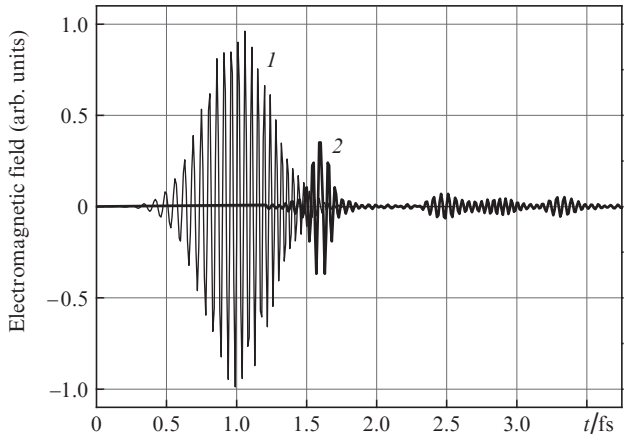

Figure 7. Comparison of the fields of the incident pulse (*1*) and the pulse reflected from the AMM (*2*) with randomised layer-thickness distribution.

3.3. Effect of molybdenum film density

The third factor that affects the reflection coefficients of multilayer mirrors is the deviation of thin-film densities from the tabular values for massive materials. An analysis of the characteristics of PMMs suggests that the greatest effect on the reflectivity of classical mirrors composed of materials with strongly different atomic numbers is exerted by the density of the heavy material (the scatterer), while the density of the light material is approximately equal to the tabular value. It is also well known that the density of scatterer films depends on their thickness [21]. This problem has been best studied for the Mo/Si mirrors intended for the 13.5-nm spectral domain [22, 23]. However, these investigations were performed for a narrow range of molybdenum film thicknesses. For AMMs the thickness range is considerably broader, which invited additional investigations.

For this purpose, use was made of a set Mo/Si PMMs with an invariable silicon film thickness h_{Si} and a molybdenum film thickness h_{Mo}, which was varied in the 1.5–5.5 nm range. The samples were made by magnetron sputtering technique in the atmosphere of argon at a pressure of 1×10^{-3} Torr. The growth conditions of the Mo/Si PMMs are described in greater detail in Ref. [24]. Their substrates were silicon plates employed in microelectronic industry, which had an effective roughness of 0.3 nm measured by atomic-force microscopy and low-angle X-ray scattering techniques with the use of the equipment and methods described in Refs [25, 26].

The structural parameters of the samples were determined by fitting experimental angular dependences of 0.154-nm reflectivities to the calculated ones. The measurements were carried out with a four-crystal high-resolution PANalytical X'Pert Pro diffractometer [18]. To decrease the number of parameters and, accordingly, improve the accuracy of measurements from the reflectivity curve, for further measurements we selected samples devoid of fluctuations and systematic period variations (the samples were identified from the absence of broadening of Bragg reflection peaks). The fit parameters were the period, the film thicknesses h_{Si} and h_{Mo} in the period, and the interlayer roughness at different interfaces. An example of such a fitting is provided by Fig. 8. From an analysis of different realisations the uncertainty of molybdenum density measurements is estimated at ±2%. The measured data are shown in Fig. 9.

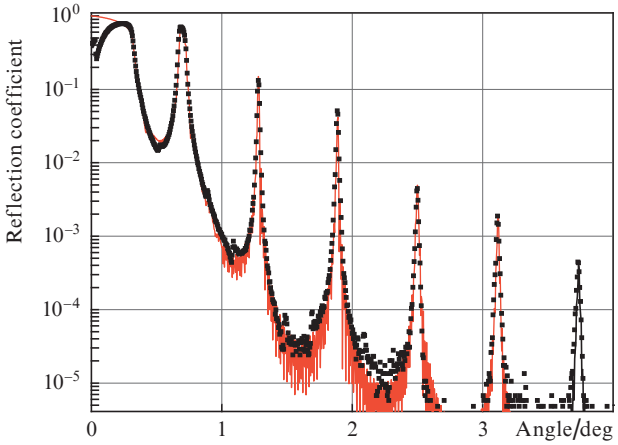

Figure 8. Example of fitting the data of low-angle X-ray diffraction for Mo/Si PMMs. Experimental data are indicated by points and the solid curve stands for the theoretical fitting.

With reference to Fig. 2, in our AMM designed for compressing femtosecond pulse the thickness of molybdenum films varies between 2.1 and 5.2 nm. According to Fig. 9, the density of Mo films varies in a range of 0.77–0.97 of the tabular value. Therefore, correct calculations require varying not only the thickness of molybdenum films but also their

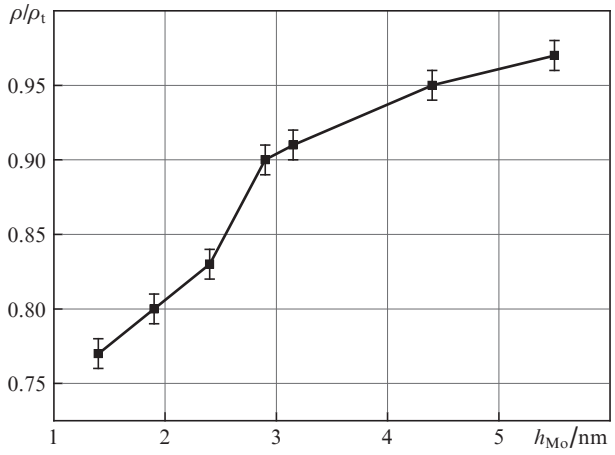

Figure 9. Mo film density ρ normalised to the tabular value ρ_t and plotted as a function of the film thickness in a Mo/Si PMM.

density in relation to their thickness. However, the structure optimisation problem with so large a parameter set has never been solved, to date. That is why to estimate the effect of molybdenum layer density on the amplitude and phase of the complex reflection coefficient of an AMM we considered the cases when the densities of every layer of a specific AMM are equal but are different for different AMMs. Shown in Figs 10a and 10b are the data calculated for molybdenum densities of 1, 0.95, 0.9, 0.85, 0.8, and 0.7 of the tabular value. One can see that the departure of molybdenum film density from the tabular value affects both the phase and amplitude of the reflection coefficient. In this case, the difference from the ideal case becomes stronger as the departure increases. In particular, a 10% decrease in density results in an almost two-fold lowering of the amplitude of reflected pulses and its lengthening by nearly a factor of 1.5 (see Table 1). And when it is considered that Mo film densities within one AMM vary in the range 77%–97% of the tabular value, depending on the film thickness, it is valid to say that design and experimental AMM characteristics will be much different. Therefore, an adequate design of the optimal AMM structure calls for the inclusion of the thickness dependence of the film density directly in the course of optimisation.

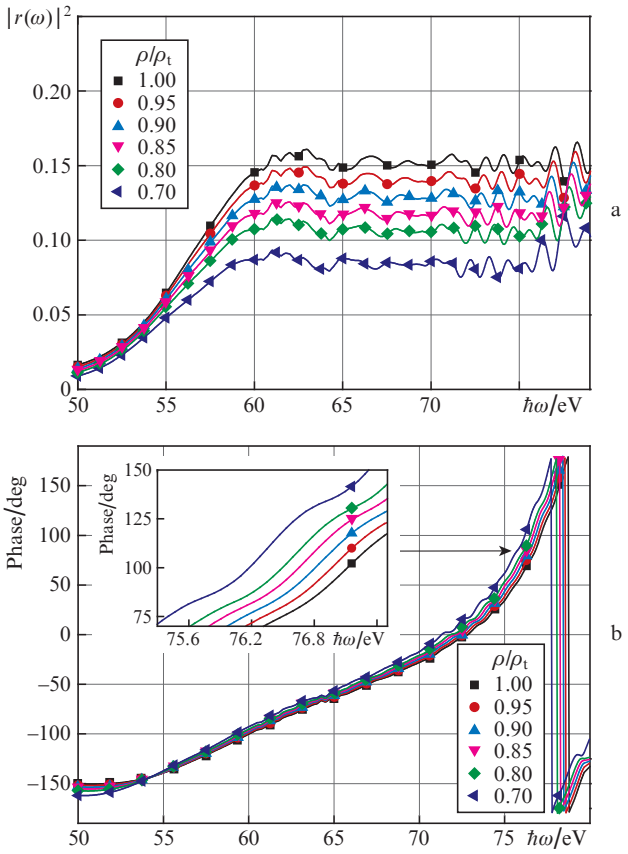

Figure 10. (Colour online) Effect of molybdenum density deviation from the tabular value on the squared amplitude (a) and phase (b) of the complex reflection coefficient of the AMM.

4. Conclusions

By the example of a model Mo/Si AMM intended for compressing chirped pulses, here we pioneered a numerical study of the effect of structural AMM imperfections (interlayer roughness, layer thickness fluctuations, and deviations of Mo film densities from the tabular one) on the amplitude and phase of the complex reflection coefficient as well as on the amplitude and duration of reflected pulses. The following results were obtained in the course of our analysis.

First, the deviations of Mo film density from the tabular value and film thickness fluctuations were shown to exert the strongest effect on the amplitude and duration of reflected pulses. The interlayer roughness exerts a comparable effect on the amplitude of the reflection coefficient but its effect on the pulse duration is moderate (it increases the duration by about 10%).

Second, in the practical application of AMMs the fluctuations of film density even at a level of 1% of layer thickness may give rise to strong adverse effects, in particular to the appearance of additional high-intensity pulses delayed in time relative to the main pulse. That is why improving the AMM fabrication technology calls for the development of techniques that will make it possible to study in laboratory conditions the spectral dependences of the amplitude and phase of the reflection coefficient in order to predict the effect of an AMM on the characteristics of reflected pulses.

Third, the strong effect of Mo film density on the intensity and duration of reflected pulses along with the thickness dependence of the film density underlies the unpredictability of the properties of AMMs designed with neglect of this factor. Development of AMM structure optimisation algorithms (programmes) that would take this dependence into account is therefore a topical task for the near future.

Fourth, for the first time the thickness dependence of Mo film density in Mo/Si PMMs was measured in a broad thickness range (1.5–5.5 nm). The density was shown to vary from 0.77 to 0.97 (in fractions of the tabular value for massive molybdenum) with film thickness variation from 1.5 to 5.5 nm. This result is of interest not only for AMMs but also for PMMs intended for operation in the long-wavelength part of the EUV range ($\lambda > 13.5$ nm), when the molybdenum film densities in PMMs and AMMs are comparable.

Acknowledgements. This work was supported by the Presidium of the Russian Academy of Sciences (Programme 'Extreme laser radiation: physics and fundamental applications'), the Russian Foundation for Basic Research (Grant No. 17-52-150006), as well as by the RSF–DFG (Grant No. 16-42-01034) with respect to determination of the thickness dependence of molybdenum film density.

References

1. Ivanov A.A., Alfimov M.V., Zheltikov A.M. *Phys. Usp.*, **47** (7), 687 (2004) [*Usp. Fiz. Nauk*, **174** (7), 743 (2004)].
2. Luo W., Yu T.P., Chen V. *Opt. Express*, **23** (6), 7732 (2015).
3. Yeung M., Rykovanov S., Bierbach J. *Nat. Photonics*, **11**, 32 (2017).
4. Kryukov P.G. *Phys. Usp.*, **58** (8), 762 (2015) [*Usp. Fiz. Nauk*, **185** (8), 817 (2015)].
5. Squier J.A., Muller M., Brakenhoff G.J., et al. *Opt. Express*, **3** (9), 315 (1998).
6. Hentschel M., Kienberger R., Spielmann Ch., et al. *Nature*, **414**, 509 (2001).
7. Barysheva M.M., Pestov A.E., Salashchenko N.N., et al. *Phys. Usp.*, **55** (7), 681 (2012) [*Usp. Fiz. Nauk*, **182** (7), 727 (2012)].
8. Saldin E.L., Schneidmiller E.A., Yurkov M.V. *New J. Phys.*, **12**, 035010 (2010).
9. Bourassin-Bouchet C., de Rossi S., Wang J. *New J. Phys.*, **14**, 023040 (2012).

10. Lin C.-Y., Yin L., Chen S.-J., et al. *Chin. Phys. B*, **25** (9), 097802 (2016).
11. Morlens A.-S., Balcou P., Zeitoun P., et al. *Opt. Lett.*, **30** (12), 1554 (2005).
12. Wonisch A., Neuhäusler U., Kabachnik N.M., et al. *Appl. Opt.*, **45** (17), 4147 (2006).
13. Guggenmos A., Hofstetter M., Rauhut R., et al. *Proc. SPIE*, **8502**, 850204 (2012).
14. Beigman I.L., Pirozhkov A.S., Ragozin E.N. *JETP Lett.*, **74** (3), 149 (2001) [*Pis'ma Zh. Eksp. Teor. Fiz.*, **74** (3), 167 (2001)].
15. Ragozin E.N., Kondratenko V.V., Levashov V.E., et al. *Proc. SPIE*, **4782**, 176 (2002).
16. Gaikovich P.K., Polkovnikov V.N., Salashchenko N.N., et al. *Quantum. Electron.*, **46** (5), 406 (2016) [*Kvantovaya Electron.*, **46** (5), 406 (2016)].
17. Beigman I.L., Pirozhkov A.S., Ragozin E.N. *J. Opt. A: Pure Appl. Opt.*, **4** (4), 443 (2002).
18. Windt D.L. *Comput. Phys.*, **12** (4), 360 (1998).
19. Aquila A.L., Salmassi F., Dollar F., et al. *Opt. Express*, **14** (21), 10073 (2006).
20. Kuhlmann T., Yulin S., Feigl T., et al. *Proc. SPIE*, **4782**, 196 (2002).
21. Chernov V.A., Chkhalo N.I., Fedorchenko M.V., et al. *J. X-Ray Sci. Technol.*, **5** (4), 389 (1995).
22. Stearns M.B., Chang C., Stearns D.G. *J. Appl. Phys.*, **71**, 187 (1992).
23. Andreev S.S., Gaponov S.V., Gusev S.A. *Thin Solid Films*, **415**, 123 (2002).
24. Andreev S.S., Akhsakhalyan A.D., Bibishkin M.A. *Centr. Eur. J. Phys.*, **1**, 191 (2003).
25. Chkhalo N.I., Churin S.A., Pestov A.E., et al. *Opt. Express*, **22** (17), 20094 (2014).
26. Chkhalo N.I., Salashchenko N.N., Zorina M.V. *Rev. Sci. Instrum.*, **86**, 016102 (2015).